Main Manuscript for

Molecular insights into substrate recognition and discrimination by the N-terminal domain of Lon AAA+ protease

Authors: Shiou-Ru Tzeng[1*], Yin-Chu Tseng[1], Chien-Chu Lin[2,5], Chia-Ying Hsu[1], Shing-Jong Huang[3], Yi-Ting Kuo[1], Chung-I Chang[2,4*]

Affiliations:

1. Institute of Biochemistry and Molecular Biology, College of Medicine, National Taiwan University, Taipei, Taiwan.
2. Institute of Biological Chemistry, Academia Sinica, Taipei 11529
3. Instrumentation Center, National Taiwan University
4. Institute of Biochemical Sciences, College of Life Science, National Taiwan University, Taipei, 10617 Taiwan
5. Present Address: Institute of Molecular Biology, Academia Sinica, Taipei 11529, Taiwan

***Corresponding authors**

Shiou-Ru Tzeng: R907, No. 1 Jen- Ai Road Section 1, Taipei 10051, Taiwan.; TEL: (+886)-22312-3456 ext 88205; FAX: (+886)-2239-15295; E-mail: srtzeng@ntu.edu.tw

Chung-I Chang: 128, Section 2, Academia Road, Nankang 11529, Taipei, Taiwan.; TEL: (+886)-22785-5696 ext 7110; E-mail: chungi@gate.sinica.edu.tw

Keywords

Lon AAA+ protease; N-terminal domain; degrons; misfolded proteins; protein aggregates; *Meiothermus taiwanensis*.

This PDF file includes:

Main Text

Table 1

Figures 1 to 7

Abstract

The Lon AAA+ proteases (LonA) is a ubiquitous ATP-dependent proteolytic machine, which selectively degrades damaged proteins or native proteins carrying exposed motifs (degrons). Here we characterize the structural basis for substrate recognition and discrimination by the N-terminal domain (NTD) of LonA.

The results reveal that the six NTDs are attached to the hexameric LonA chamber by flexible linkers such that the formers tumble independently of the latter. Further spectral analyses show that the NTD selectively interacts with unfolded proteins, protein aggregates, and degron-tagged proteins by two hydrophobic patches of its N-lobe, but not intrinsically disordered substrate, α-casein. Moreover, the NTD selectively binds to protein substrates when they are thermally induced to adopt unfolded conformations. Collectively, our findings demonstrate that NTDs enable LonA to perform protein quality control to selectively degrade proteins in damaged states and suggest that substrate discrimination and selective degradation by LonA are mediated by multiple NTD interactions.

Impact Statement

The N-terminal domains enable Lon protease to discriminate and capture selected protein species for degradation by exposed hydrophobic patches and flexible linkages to the hexameric core complex.

Introduction:

The Lon AAA+ protease (LonA), previously known as the protease La, is an ATP-dependent protease distributed in prokaryote and eukaryote[1]. It forms a homo-hexamer to execute its biological function[2,3]. LonA belongs to the AAA+ (ATPases associated with various cellular activities) superfamily and contains an N-terminal domain (NTD), a middle ATPase domain with conserved Walker motifs for ATP hydrolysis, and a C-terminal protease domain (CTD) with a serine-lysine catalytic dyad in the active site[4,5]. LonA is responsible for degrading damaged or unfolded proteins, as well as native proteins bearing specific recognition elements, known as degradation tag or degrons[6,7]. How can LonA discriminate its substrate from other non-substrate proteins in a cell? Substrate recognition of LonA is thought to be mediated by its NTD[8-14]. The substrates are unfolded and translocated in an ATP-dependent process into a secluded chamber formed by the ATPase domains and the protease domains. Finally, the unfolded substrates inside the chamber are degraded into small peptide fragments[15,16]. The ATP-dependent translocation process of substrates into the hexameric chamber, formed by the AAA+ and protease domains, has been well characterized[17,18]. Structures of different N-terminal fragments of LonA from three species have been reported[19-22], including *Escherichia coli* (EcLon), *Mycobacterium*

64 *avium complex* (MacLon) and *Bacillus subtilis* (BsLon). However, no structural study has been conducted
65 to analyze substrate interaction by the NTD either in isolation or in the context of full-length LonA.
66 Here we address the question of substrate recognition and discrimination by the NTD domains of
67 LonA using nuclear magnetic resonance (NMR) spectroscopy. To understand how LonA selectively
68 recognizes protein substrates being in damaged states, we have used a thermal stable LonA isolated
69 from *Meiothermus taiwanensis* (termed MtaLonA henceforth), which allows temperature cycling
70 experiments to be applied to change the populations of a protein substrate in folded and unfolded states.
71 In this work, five various protein substrates have been employed for NMR experiments, which include: (i)
72 Ig2 (domains 5 and 6 of the gelation factor from *Dictyostelium discoideum*[23], hereafter abbreviated as Ig2)
73 with an immunoglobulin (Ig) fold forming a dimer that is natively folded up to 40 °C; (ii) α-casein, which is
74 an intrinsically disordered protein with no tertiary structure; (iii) native lysozyme with four disulfide
75 bridges and reduced lysozyme forming loose and flexible aggregates; (iv) Ig2D5 (domain 5 of the
76 gelation factor from *Dictyostelium discoideum*), which is used for characterization of substrate
77 conformation selection by NTD; and (v) a degron-tagged Ig2D5 designed to identify the residues of
78 degrons that are recognized and bound by NTD.
79 Here we show that the presence of NTD is required to degrade damaged proteins and native
80 proteins with degrons, but it does not play an active role in mediating the degradation by LonA of an
81 intrinsically disordered substrate, α-casein. We have also determined the crystal structure of an N-
82 terminal fragment of MtaLonA, and refined it to 2.1 Å resolution. The structure is homologous to the
83 structures of N-terminal fragment of both EcLon and MacLon[19-22] , but not to that of BsLon[20]. With the aid
84 of perdeuteration labeling and transverse relaxation optimized NMR spectroscopy (TROSY), we find that
85 the NTD appears to tumble independently of the hexameric core complex, suggesting that the NTD is
86 attached to the hexameric chamber by a flexible linker thus rendering it possible for detailed chemical
87 shift perturbation mapping of substrate binding in the context of full-length MtaLonA. We further
88 structurally characterize the NTD-mediated interactions with unfolded proteins, protein aggregates, or
89 degron-tagged proteins to elucidate its functional role in substrate discrimination. Our results demonstrate
90 that the substrate-binding site of NTD is located at hydrophobic patches of its N-lobe, which recognizes
91 exposed aromatic and hydrophobic residues of damaged proteins and degrons. Using temperature

92 cycling experiments, we investigate how the conformations of substrates are affected in the presence of
93 MtaLonA NTDs, which interact with the initial substrate before subsequent translocation and degradation.
94 Altogether, this work elucidates the substrate recognition mediated by the NTDs of MtaLonA at
95 substantially high resolution and suggests that the flexibly linked NTDs can help survey, discriminate, and
96 selectively capture damaged unfolded protein species or native protein substrates carrying exposed
97 degradation sequence motifs.
98
99 **Results**
100 ***The NTD is essential for efficient degradation of a thermally unfolded substrate but not***
101 ***intrinsically disordered protein substrate*, *α-casein.***
102 To evaluate the importance of the NTD in the proteolysis activity of MtaLonA, we constructed a
103 MtaLonA variant, AAAP, of which the NTD (residues 1-241) was removed (Fig. 1A), based on the
104 structure of *B. subtilis* LonA. Substrate degradation activity of full-length MtaLonA and AAAP were
105 evaluated using two protein substrates, namely α-casein and Ig2. Native α-casein is an intrinsically
106 disordered substrate of LonA. Ig2 is an all β-stranded protein that becomes partially unfolded at 55 °C
107 (supplementary Fig. 1A) and only then is susceptible to proteolysis by MtaLonA[6]. Full-length MtaLonA
108 degrades both α-casein as well as Ig2[24]. Compared to the full-length MtaLonA, AAAP exhibits a slightly
109 reduced degradation activity against α-casein (Fig. 1B) while its proteolytic activity for Ig2 is severely
110 impaired (Fig. 1C). These results showed that, despite the lack of the NTD, AAAP retains the proteolytic
111 activity for intrinsically disordered protein substrates like α-casein. However, the NTD is essential for
112 MtaLonA to recognize and degrade the thermally damaged substrate, Ig2, indicating the NTD may
113 mediate specific interactions with damaged Ig2 but not α-casein.
114 ***The NTDs tumble independently of the hexameric LonA core in solution***
115 We obtained crystals of the N-terminal fragment NN206 of MtaLonA by *in situ* proteolysis during
116 crystallization (Fig. 2A). The structure was refined to 2.1 Å resolution with a free R factor of 24.9%
117 (crystallographic R factor is 20.9%) (Table 1). NN206 forms a bilobal fold: (i) the N-terminal lobe, which
118 consist of one α-helix and six β-strands, forming three β-sheets (β1/β3/β4/β5, β2/β5/β4 and β1/β6/β5); (ii)
119 the C-terminal lobe, which is is exclusively α-helical, consisting of a five-helix bundle (Figs. 2B). The two

120 lobes are jointed together by an 18-residue linker, which is similar to that of both EcLon and MacLon[19-22].
121 Based on the result, we also crystallized and solved the structure of the longer N-terminal fragment
122 NN291 (Fig. 2A). The structure of NN291 was refined to 1.7 Å resolution (Table 1), which is similar to
123 NN206 except for a longer C-terminal helix by 4 more residues, i.e., residues 207-210 (Fig. 2C). Despite
124 the lack of spontaneous proteolytic fragmentation in the crystals, no electron density was seen past
125 residue A210 (Fig. 2D).

126 Interestingly, the C-terminus of *E. coli* N-terminal fragment forms an extended 40-residue helix[21].
127 Therefore, we further investigate the structural feature of the corresponding residues 207-243 of MtaLonA
128 using solution-state NMR spectroscopy. Most of the well-dispersed cross-peaks in the two-dimensional
129 ^{15}N-^{1}H HSQC NMR spectra of NN206 and NN243 can be superimposed, indicating that the well-folded
130 domain structure corresponding to residues 1-206 is not perturbed by the C-terminal extension, residues
131 207-243 (Fig. 2E). Nonetheless, NN243 exhibits extra intense and poorly dispersed cross-peaks around
132 7.5-8.5 ppm along the proton dimension that is indicative of a highly disordered peptide segment, which
133 most likely corresponds to the C-terminal extension of NN243. Together, our crystallographic and NMR
134 analyses suggest that the N-terminal domain of MtaLonA forms a bilobal globular structure (residues 1-
135 206) followed by a C-terminal flexible extension (residues 211-243).

136 LonA forms a large homo-hexameric complex resulting in a very high molecular weight of 0.5
137 MDa. To verify the dynamic feature of the NTD, we compared the backbone amide ^{15}N-^{1}H NMR
138 correlations of NN206 and those of full-length MtaLonA at 55 ºC. With the aid of perdeuteration labeling
139 and transverse relaxation optimized NMR spectroscopy (TROSY), we could observe over 200 well-
140 resolved ^{15}N-^{1}H correlations of full-length hexameric MtaLonA at an apparent molecular weight of 0.5
141 MDa. Importantly, most of these correlations are superimposable to those observed in the NN206
142 spectrum (Fig. 2F). These results indicate that the NTD adopts the same structure as the isolated NTD
143 while loosely tethered to the near-megadalton hexameric LonA core via a long flexible linker thus leading
144 to an independent, fast tumbling motion to yield highly favorable NMR relaxation properties and thus high-
145 quality multidimensional NMR spectra. We further applied multidimensional heteronuclear NMR
146 experiments to assign the observed cross peaks in the ^{1}H–^{15}N TROSY HSQC spectrum of NN206
147 (supplementary Fig. 2). Together, these results suggest that in a LonA complex, the six N-terminal

148 domains may each connect to the hexameric core of fused AAA+ and protease domains by flexible ~40-
149 residue linkers. Therefore, each of the six 24-kDa N-terminal domains may tumble independently of the
150 350-kDa hexameric core (Fig. 2G).

151 ***The chemical shifts of NTDs are perturbed by thermally unfolded proteins, aggregates, and***
152 ***degron tags***

153 To directly observe discrimination of native or thermally damaged substrate mediated by NTD, we
154 treated NMR samples by a thermal cycle with temperature increasing from 32 °C to 55 °C and then
155 returning to 32 °C. With temperature rising, the exposed hydrophobic areas of thermally unfolded Ig2 is
156 increased, as detected by SYPRO Orange (supplementary Fig. 1A), indicating that the population of Ig2
157 in unfolded states is increased by thermal denaturation. By contrast, thermal cycling of isolated NTDs
158 exhibited no temperature effect on protein structure monitored by NMR spectroscopy, which may be
159 explained by the high melting temperature (T_m) of full-length MtaLonA and NN206 (68.0 °C and 85.5 °C,
160 respectively; supplementary Figs. 1A and 1B). Upon addition of a 2-fold molar excess of well-folded Ig2 at
161 32 °C, no significant chemical shift perturbation (CSP) is observed (Fig. 3A), where only the NTD is
162 isotopically enriched. By increasing temperature from 32 °C to 55 °C for the same NMR sample, a
163 dramatic variation in the 2D spectral features is detected and the resonances undergo a prominent
164 decrease in intensity (Fig. 3B), indicating that the NTD interacts with thermally unfolded Ig2. With
165 temperature dropping from 55 °C to 32 °C, line width of the expected bound-state resonances is too
166 broad to be detected in the presence of binding events (Fig. 3C), suggesting a certain portion of Ig2 still
167 stays in the unfolded or aggregated state. In contrast, the addition of α-casein results in little to no effect
168 on the cross-peaks of residues 1-206 of the NTD (supplementary Fig. 3) thus precluding specific
169 interaction mode between the intrinsically disordered protein α-casein with the NTD of MtaLonA.

170 To clarify whether overall broadening of the cross-peak signals is due to protein aggregation or
171 precipitation, we performed size-exclusion chromatography (SEC) experiments to examine the NMR
172 sample treated with thermal cycling. The analysis revealed that more than half of Ig2 protein becomes
173 unfolded and aggregated through a thermal cycle while the NTD is still well-folded (Fig. 3D). The NTD-Ig2
174 aggregate complex showed a dissociable SEC profile, suggesting the NTD-substrate interaction is quite
175 dynamic by nature and the fast substrate dissociation may facilitate the translocation process.

176 NMR analysis indicated that thermally damaged Ig2 induced significant CSPs and broadened
177 resonances in the NTD N-lobe, which comprise one α-helix and three β-sheets β1/β3/β4/β5, β2/β5/β4
178 and β1/β6/β5. The residues of NTD with the pronounced CSPs are part of the interaction interface
179 located mainly at helix α1, loop L1, L2, L3 and β-sheet β2/β5/β4 (Figs. 3E and 3F), which consist primarily
180 of hydrophobic residues and are decorated by a number of polar residues (supplementary Fig. 4A). To
181 characterize the binding sites of the NTD interaction with damaged Ig2, we chose to mutate two exposed
182 hydrophobic residues Pro-22 and Met-85 located at the center of β-sheet β2/β5/β4, which form a
183 contiguous hydrophobic surface in the N-lobe subdomain (Fig. 3G and supplementary Fig. 4B). We found
184 that NN206*, containing two specific mutations in the NTD (P22A and M85A; hereafter NN206*), may
185 influence the hydrophobic substrate-binding interaction. The NMR sample containing both NN206* and
186 Ig2 protein was also treated with one thermal cycle. NN206* showed much weak interactions with
187 thermal damaged Ig2 (Figs. 3H-J), confirming that this binding event is mainly contributed by the specific
188 hydrophobic residues with high hydrophobicity in a continuous hydrophobic surface of the N-lobe.
189 Collectively, our results show that the NTD of LonA selectively interacts with protein substrates, via critical
190 bulky hydrophobic residues on the hydrophobic surface of its N-lobe, demonstrating that NTD enables
191 LonA to perform protein quality control by selectively interacting with proteins in damaged or unfolded
192 states.
193 To further examine how the NTD is involved with protein aggregation, we probed the interactions
194 between the scrambled lysozyme aggregate and MtaLonA NTD by NMR spectroscopy. Native lysozyme
195 is a 14.3-kDa protein (129 amino acids) comprising four disulfide bridges while reduced lysozyme
196 forms loose and flexible aggregates[25]. TCEP (tris (2-carboxyethyl) phosphine; nonthiol-based reducing
197 agent) drives the formation of amorphous lysozyme aggregates observed in this study. Moreover, there is
198 no cysteine residue found in full-length MtaLonA, suggesting TCEP does not affect the structure of NTD.
199 Addition of TCEP-treated denatured lysozymes leaded to substantial spectral changes of NN206
200 resonances recorded at 32 °C while NN206* showed marginal CSPs marginal CSPs (supplementary Fig.
201 5A). The structural mapping shows that the affected residues caused by TCEP-treated denatured
202 lysozyme are also located mainly in the N-lobe shown in supplementary Figs. 5B and C. Furthermore, we
203 also examined the degradation activity of LonA against either native or denatured lysozyme, respectively.

204 A gel-based assay showed that full-length MtaLonA can efficiently degrade denatured-reduced lysozyme,
205 but not native lysozyme (supplementary Fig. 5D). Accordingly, AAAP, without the NTD, was inactive
206 against either the scrambled lysozyme aggregate or native lysozyme (supplementary Fig. 5E). Together,
207 these results highlight the key role of NTD, via the N-lobe region, in discriminating and recognizing protein
208 aggregates before subsequent translocation and degradation.

209 LonA can also degrade natively folded proteins with degradation tags such as sul20 degron[6,26].
210 Previously, the NTD of *E. coli* LonA was shown to be required for degron binding by chemical cross-
211 linking[7]. To understand how the NTD directly interacts with degrons, a 20-residue peptide (the C-terminal
212 20 residues of SulA; namely Sul20)[7] is synthesized and used for NMR titration experiments. Addition of
213 equimolar unlabeled Sul20 causes significant spectral changes of NN206 resonances (Fig. 4A) and the
214 structural mapping shows that the affected residues are again located at β-sheet β2/β5/β4, loop L1, L3
215 and helix α1 of the N-lobe subdomain (Fig. 4B). Mutations of P22 and M85 located at the center of the
216 hydrophobic surface to moderately hydrophobic Ala lead to much weak interactions of NN206* with Sul20
217 peptide (supplementary Fig. 6A), suggesting that specific hydrophobic residues of beta-stranded
218 β2/β5/β4 located at the N-lobe of MtaLon NTD play a critical role on degrons recognition.

219 To characterize the effect of MtaLon NTD on degrons further, we appended Sul20 to the C terminus
220 of a protein substrate Ig2D5 (domains 5 of the gelation factor from *Dictyostelium discoideum*, hereafter
221 abbreviated as Ig2D5) and investigated the conformational changes experienced by Sul20 upon binding
222 the NTD. The NMR spectra of Ig2D5 and Ig2D5-S20 can be well superimposed, indicating that the well-
223 folded domain structure corresponding to Ig2D5 is not perturbed by the C-terminal Sul20 (Fig. 4C).
224 Furthermore, Ig2D5-S20 exhibits additional cross-peaks that well correspond to Sul20. Elevated [^{1}H]–^{15}N
225 nuclear Overhauser effect (NOE) values for most residues are from Ig2D5 (Fig. 4D), along with the large
226 increase in chemical shift dispersion. Lower [^{1}H]–^{15}N NOEs for Sul20 residues are due to the increased
227 flexibility on ps-ns timescale. By addition of the unlabeled NN206 to isotopically enriched Ig2D5-S20, we
228 observed chemical shift changes and broadened resonances of C-terminal Sul20 (Figs. 4E and 4F),
229 suggesting that residues Y19 and H20 are strongly affected by the binding event based on the resonance
230 broadening beyond detection. The NMR spectrum of Ig2D5-S20 in the presence of an equimolar amount
231 of unlabeled NN206* shows a much less pronounced chemical shift effect (supplementary Fig. 6B) than

232 wild-type NN206 binding to Ig2D5-S20, indicating that Sul20 tag can be recognized by the hydrophobic
233 patches of N-lobe of MtaLon NTD.

234 ***The thermally unfolded conformations of substrate proteins are stabilized by engagement with***
235 ***NTDs.***

236 To understand further selective recognition of protein substrate in the unfolded states by the NTD,
237 we ask whether the unfolding-refolding process of protein may be modulated by interacting with the NTD.
238 To investigate how the conformations of substrates are influenced in the presence of NTDs, we
239 constructed a single-domain protein substrate Ig2D5 (domains 5 of the gelation factor from *Dictyostelium*
240 *discoideum*) for NMR experiments due to its high-quality NMR spectrum (supplementary Fig. 7A). About
241 96% of the backbone resonances of Ig2D5 can be assigned by multidimensional heteronuclear NMR
242 experiments. Ig2D5 is a β-sheet protein with Ig-like fold and the T_m of substrate Ig2D5 is similar to Ig2
243 (supplementary Figs. 7B and 7C). Here we applied NMR spectroscopy to investigate unfolding-refolding
244 equilibria of the substrate Ig2D5 induced by temperature cycling while MtaLon NTD remains stable
245 through the entire temperature cycling. The NMR samples containing isotopically enriched Ig2D5 in the
246 absence and presence of unlabeled NN206 were heated from 32 ºC to 60 ºC and then cooled to 32 ºC.
247 Based on the intensity changes of resonances corresponding to native Ig2D5, we estimated that isolated
248 Ig2D5 is largely unfolded at 60 ºC (Figs. 5A and B; the spectra are shown in green) and ~72% becomes
249 folded after a thermal cycling (Fig. 5C). However, in the presence of equimolar NN206, less than 15%
250 Ig2D5 is folded after one thermal cycle (Figs. 5C; the spectrum is shown in blue). Similar results were
251 obtained using equimolar full-length MtaLonA catalytic mutant S678A (LonA*) (Figs. 5C; the spectrum is
252 shown in red). However, addition of equimolar AAAP* (residues 242-793 with catalytic mutant S678A),
253 Ig2D5 is largely unfolded at 60 ºC (Fig. 5B; the spectrum is shown in black) and ~75% becomes folded
254 after thermal cycling (Fig. 5C; the spectrum is in black). The results reveal that the unfolded state of
255 Ig2D5 is engaged with MtaLon NTD and the temperature-induced unfolding-refolding of substrate is
256 significantly affected in the presence of MtaLon NTDs (Fig. 5D), potentially priming it for subsequent
257 translocation process. Accordingly, we also examined how the unfolding-refolding of Ig2D5 can be
258 affected by NN206*. After one thermal cycle, about 75% of Ig2D5 becomes folded in the presence of
259 equimolar NN206* (Fig. 5E and supplementary Figs. 7D, E and F). Upon addition of eightfold excess of

260 NN206*, about 45% of Ig2D5 becomes folded, suggesting that NN206* interacts with denatured protein
261 substrate weakly. These results demonstrate that the conformations of substrate are affected by the
262 hydrophobic substrate-binding interaction and the thermally unfolded states of substrate proteins can be
263 stabilized by engagement with the NTDs. Thus, by selectively interacting with hydrophobic residues
264 exposed in the thermally unfolded states of substrate proteins NTDs prominently perturb temperature-
265 induced unfolding-refolding process of substrate.
266
267 **Discussion**
268 In this work we used α-casein and Ig2, which represent two types of substrates. Native α-casein
269 is an intrinsically disordered protein; by contrast, the native Ig2 is a β-sheet protein with T_m at 46 °C
270 (Supplementary Fig. 1). We show that the construct AAAP devoid of the NTD (residues 242-793, ATPase
271 and protease domains), which retains wild-type ATPase and peptidase activities in LonA, lacks the
272 degradation activity against thermally denatured Ig2 while exhibits a wild-type-like activity against α-
273 casein (Fig.1). Therefore, the NTD is specific for denatured or damaged protein substrates, whose
274 hydrophobic core regions normally buried in the folded state become exposed, but not for intrinsically
275 disordered substrates like casein, which contains mainly charged or polar residues and lack hydrophobic
276 regions in the protein sequence. Indeed, it has been shown that LonA prefers substrates rich in
277 hydrophobic residues[26].
278 Our crystallographic results of NN206 and NN291 are consistent with previous findings that the
279 ~40-residue region between the NTD and ATPase-Protease domains is structurally flexible with multiple
280 accessible protease sites[9,20,27,28]. This notion is also corroborated by our high-resolution NMR analyses
281 on the NTD both in isolation and as a part of the full-length protein, demonstrating the independent, fast
282 tumbling motion of the NTDs in the ~0.5 MDa hexameric assembly of LonA. Moreover, their highly
283 favorable NMR relaxation properties and resulting high-quality multidimensional NMR spectra have
284 allowed us to analyze the interaction of the NTD with unfolded proteins, protein aggregates, degron tags,
285 and intrinsically disordered substrates. Our work provides atomic details of the NTD-mediated substrate
286 discrimination by temperature-based switching of the native folded protein to its unfolded state in an NMR
287 sample. NMR characterization indicates NTD does not interact with well-folded Ig2, native lysozyme or

288 intrinsically disordered α-casein, whereas unfolded proteins, aggregates and degron tags can elicit
289 pronounced chemical shift changes to the N-lobe of the NTD, which is subsequently confirmed by
290 structure-based mutagenesis. Collectively, these results suggests that LonA has two substrate-interacting
291 modes: (1) the NTD-non-requiring mode for intrinsically disordered substrates lacking hydrophobic-rich
292 region, which may be engaged directly with the pore-loops in the LonA assembly without involving the six
293 NTDs; (2) the NTD-requiring mode for recognizing and trapping damaged/denatured protein substrates
294 with exposed hydrophobic regions before their engagement with the pore-loops of the LonA assembly.
295 The key role of NTD is to enable LonA to perform protein quality control to selectively capture and
296 degrade proteins in damaged unfolded states.

297 By analyzing the NTD of MtaLonA interactions with damaged Ig2, the scrambled lysozyme and
298 Sul 20 peptide, we conclude that these binding events are mediated by two hydrophobic patches, which
299 comprise (i) Leu-10, Ile-15, Pro-22, Val-23, and Met-85 (termed hpI in the following) ; (ii) Met-75, Leu-77,
300 Pro-78 and Leu-82 (termed hpII) (Fig. 6A). Our results also demonstrate that a double mutant NN206*
301 (Pro-22 and Met-85 replaced by Ala), resulting in decreased hydrophobicity of hpI, has a significant effect
302 on the ability of MtaLonA NTD to bind to damaged or misfolded proteins, indicating that the bulky
303 hydrophobic residues on hydrophobic patches are essential determinants for substrate recognition and
304 discrimination. We also examine the exposed hydrophobic residues of β-sheet β2/β5/β4, loop L1 and loop
305 L3 located at the N-lobes of other reported structures of LonA NTDs[19-22]. The N-terminal fragment from *B.*
306 *subtilis* LonA was previously reported to adopt a domain-swapped dimer where the N-lobe of one
307 monomer is positioned next to the C-lobe of the other monomer[20]. In contrast, the structures of the N-
308 terminal fragment from MtaLon, EcLon and MacLon showed that the N- and the C-lobes are joined
309 together via a short linker (supplementary Fig. 8A and B). Based on structural alignments (supplementary
310 Fig. 8C), the N-lobe of EcLon has almost the same pattern of exposed hydrophobic residues as that of
311 MtaLon NTD (Fig. 6B). Interestingly, The NTD of MacLon shows merged hp I and II while the hpI of
312 BsLon NTD is a little distant from hpII (Figs. 6C and D). The structural comparison reveals that, similarly
313 to MtaLon NTD, all three reported structures exhibit exposed hp I and II with slight variations in their
314 shapes and sizes, suggesting that the conserved hydrophobic patches at the N-lobes may be potentially
315 responsible for conferring substrate selectivity toward degrons, misfolded and damaged proteins.

316 It has previously been known that LonA can recognize a degron-tagged protein by binding to its
317 largely exposed hydrophobic residues. Here, our results show the C-terminal Sul20 of Ig2D5-S20 has
318 substantially low heteronuclear NOE values, reflecting this region undergoes rapid local motion and is
319 solvent-exposed in solution. Therefore, NTD of MtaLonA can easily recognize and interact with the C-
320 terminal aromatic and hydrophobic residues of Sul20. This finding indicates that a pair of aromatic
321 residues consisting of Y19 and H20 in Sul20 play crucial roles in the hydrophobic interactions with
322 residues P22 and M85 of LonA NTD, which is verified with a double mutant NN206*. Residues Pro and
323 Met exhibit higher values of hydrophobicity than moderately hydrophobic Ala and mutations of both P22
324 and M85, located at the center of the contiguous hydrophobic surface, result in much weak interactions of
325 NN206* with damaged Ig2, the scrambled lysozyme and Sul20 peptide, highlighting the importance of
326 direct interaction with exposed and contiguous surface with high hydrophobicity in the recognition of
327 protein substrates by the NTD of MtaLonA. Furthermore, by selectively binding to hydrophobic residues
328 exposed in the thermally unfolded states of proteins, the NTDs prominently stabilize substrate's unfolded
329 conformation. These results show that the NTD-substrates interactions involve the hydrophobic residues
330 on both partners, suggesting aromatic and hydrophobic side chains, which are usually buried in the
331 native proteins, are important recognition determinants for the NTD to enable MtaLonA to selectively
332 capture and degrade proteins in a damaged unfolded state or with degron tags.
333 Our results directly demonstrate that thermally damaged proteins and degrons induce chemical
334 shift changes and broadened resonances located mainly in the two hydrophobic patches of N-terminal
335 lobe but we do not find evidence that the C-lobe of the NTD is involved in substrate interaction. However,
336 addition of thermally unfolded Ig2 into U-^{2}H/^{15}N-labelled full-length LonA*, affected residues are shown in
337 both N- and C-lobes of LonA* NTD at 55 °C (Figs. 7A and B). Compared ^{1}H–^{15}N TROSY HSQC spectra
338 of NN206 and MtaLonA* in the presence of thermally unfolded protein Ig2, the signals from the C-lobe of
339 MtaLonA* NTD are missing due to line broadening, suggesting others NTDs of LonA* hexamer may join
340 to interact with substrates. All together, these results reveal the free molecular tumbling of the NTD and
341 its substrate binding site, based on which a model involving multi-NTD interactions, may be proposed for
342 substrate recognition. The flexibly linked NTD of the hexametric LonA is swaying from side to side and
343 back and forth to survey, recognize, and trap substrates with exposed hydrophobic sequences (Fig. 7C).

344 After initial binding, other NTDs may join to increase the avidity of the LonA-substrate interaction (Fig.
345 7D); the engagement of a substrate protein by multiple NTDs also serves to facilitate effective substrate
346 unfolding and translocation mediated by the coordinated movements of the pore-loops in the ATPase
347 modules of the LonA chamber, powered by cycles of ATP binding and hydrolysis. Finally, the substrate
348 polypeptide chain is pulled inside the chamber and undergoes proteolysis by protease modules of LonA.
349

350 **Materials and Methods**

351 ***Peptide***

352 Sul20 peptide (Sequence: ASSHATRQLSGLKIHSNLYH) was synthesized by GenScript
353 (https://www.genscript.com/) at >95% purity.

354 ***Cloning, protein expression and purification***

355 The plasmids expressing for full-length MtaLonA (1-793 residues) or AAAP (242-793 residues) with a C-
356 terminal 6xHis-tag were transformed into *E.coli* BL21(DE3) cells[18]. Site-directed mutagenesis was
357 performed using the Quickchange kit (Stratagene). NN206 (1-206 residues), NN243 (1-243 residues) and
358 NN291 (1-291 residues) were cloned into pET-modified vector with a tobacco etch virus (TEV) cleavage
359 site. The three resultant plasmids, encoding the proteins NN206, NN243 and NN291 with the N-terminal
360 His-tag, were transformed into *E.coli* BL21(DE3) cells. The target proteins synthesis was induced with 0.5
361 mM isopropyl-thio-β-D-galactoside (IPTG) at an absorbance at 600 nm (OD_{600}) ~0.6 at 28 °C. The target
362 proteins were purified with nickel chelate affinity resins (Ni-NTA, Qiagen). The protein samples were
363 collected and purified by a Superdex 200 (GE Healthcare) column[17]. MtaLonA and AAAP proteins were
364 collected and further purified on a MonoQ (GE Healthcare) chromatography. For NN206, NN243 and
365 NN291 purification, the N-terminal His-tagged proteins were cleaved by TEV protease for overnight at 4
366 °C and then reloaded onto Ni-NTA to remove TEV protease. The flow-through fraction containing target
367 proteins were collected and purified with Superdex 75 (GE Healthcare) chromatography. Ig2 (domains 5
368 and 6 of the gelation factor ABP-120 of *Dictyostelium discoideum*)[29] and Ig2D5-S20 (Ig2 fused with
369 Sul20) were cloned into pET28a(+)tev for generation of pET28a(+)tev-Ig2 and pET28a(+)tev-Ig2D5-20.
370 The recombinant protein was induced by 0.5 mM IPTG at OD_{600} ~0.6 for 16 hours. The purifications of
371 Ig2, Ig2D5 and Ig2D5-20 is the same as NN206, NN243 and NN291. Isotopically labeled samples for

372 NMR studies were prepared by growing the cells in minimal (M9) medium. The full-length MtaLonA were
373 prepared by supplementing the growing medium with 1 g l^{-1} of $^{15}NH_4Cl$ and 4 g l^{-1} of $^{2}H_7/^{12}C_6$-glucose in
374 99.8%-$^{2}H_2O$ (Sigma-Aldrich).

375 ***Substrate degradation assays***

376 α-casein (Sigma, USA) and Ig2 were used as the substrates in these assays[17]. 4 μM substrate proteins
377 were incubated with 0.4 μM MtaLonA (hexamer) or AAAP or mutations at 55 °C. The degradation
378 reactions were halted by protein sample dye and heat inactivation at 95 °C for 5 minutes. The treated
379 reaction mixtures were then analyzed by SDS-PAGE.

380 **Protein crystallization**

381 Crystallizations of NN206 and NN291 were performed at 295K by hanging drop vapor-diffusion method.
382 For Crystallization of NN206, in situ proteolysis was performed[30]. 1 μl of MtaLonA (10 mg/ml) plus trypsin
383 in ratio 1000:1 was mixed with 1 μl of 0.1 M Tris-HCl (pH 7.5), 0.2 M Sodium acetate and 30% PEG 4000.
384 The NN206 crystals appeared in the mixed drop after 3 days. The crystals of NN291 were grown by
385 mixing with 1 μl of NN291 protein sample (15 mg/mL) and 1 μl of well solution containing 0.1 M MES (pH
386 5.8) and 0.8 M ammonium sulfate. Crystals grew to 0.2-0.3 mm over two weeks. Crystals of NN206 and
387 NN291 were cryoprotected with 20% glycerol or 20% ethylene glycol before data collection.

388 ***Structure determination***

389 The data sets of NN206 and NN291 were collected at the beamlines BL-13C1 of National Synchrotron
390 Radiation Research Center (Taiwan) and BL-1A of Photon Factory (Japan), respectively. All Data sets
391 were processed by HKL2000[31]. The structure of NN206 was solved by molecular replacement with the
392 program Phaser[32] using the structures of the N-terminal fragment of *B. subtilis* LonA (residues 4-116,
393 PDB code 3M65) and the N-terminal fragment of *E. coli* LonA (residues 120-210, PDB code 3LJC) as the
394 search models. The structure of NN291 was determined by molecular replacement using NN206
395 structure. All initial models were automatically rebuilt using the program AutoBuild[33]. Subsequently, these
396 structures were refined by manual refitting in Coot[34] and performance of refinement using the program
397 Refmac5[35]. Crystallographic and refinement statistics are listed in Table 1. All structure figures were
398 made using PyMOL (Version 1.3, Schrödinger, LLC). The atomic coordinates and structure factors for
399 NN206 and NN291 have been deposited in the Protein Data Bank (http://www.rcsb.org/) with the

400 accession numbers 7CR9 and 7CRA, respectively.

401 ***Thermal shift assay***

402 Thermal shift assay was carried out in qPCR 8-strip tubes (Gunster Biotech) using SYBRO orange (Life
403 Technologies) as dye. For each reaction, 5 μM purified MtaLonA, NN206 or Ig2 was mixed with assay
404 buffer (50 mM NaPi, 2 mM β-Me, pH 6.5) and SYPRO Orange dye (5X final concentration) in 45 μL total
405 volume/well. 100 μM Ig2D5 was mixed with assay buffer and SYPRO Orange dye (10X final
406 concentration) in 45 μL total volume/well. Samples were heated at a rate of 0.5 °C per minute from 25 °C
407 to 95 °C and fluorescence signals were recorded with the CFX Connect Real-Time PCR Detection
408 System (Bio-Rad). The melting temperatures were analyzed using the derivative plots of the melting
409 curve.

410 ***NMR spectroscopy***

411 NMR experiments were acquired on Bruker 800-MHz spectrometers (Bruker BioSpin, Karlsruhe,
412 Germany). The assignments of NN206 backbone ^{15}N, ^{1}H^{N}, ^{13}Cα, ^{13}Cβ, and ^{13}C′ chemical shifts were
413 obtained by ^{15}N-^{1}H HSQC, HNCACB, CBCA(CO)NH, HNCA, HN(CO)CA and HNCO spectra[36]. NMR
414 samples containing 50 μM [U-15N]-labeled NN206 in the absence and presence of 100 μM Ig2 are
415 prepared in the buffer: 50 mM sodium phosphate (pH 6.5) with 10% D2O. For temperature cycling
416 experiments, the first 2D ^{1}H–^{15}N TROSY HSQC spectrum was acquired at 32 °C; the same sample was
417 heated to 55 °C for recording the second spectra, and the temperature is decreased to 32 °C for
418 recording the third spectra. For characterization of substrate conformation selection by NTD, 2D ^{1}H-^{15}N
419 TROSY HSQC NMR spectra of 50 μM [U-^{15}N]-labeled Ig2D5 titrated with 50 μM unlabeled NN206,
420 MtaLonA or AAAP proteins were recorded during a thermal cycle starting from 32 to 60 °C, and then back
421 to 32 °C. 72 residues of Ig2D5 were selected for calculating folded ratio. The interaction of NN206 with
422 Sul20 peptide was recorded with 50 μM [U-15N]-labeled NN206 titrated with unlabeled 50 and 150 μM
423 unlabeled Sul20 peptide. The interaction of NN206 with TCEP-treated denatured lysozyme was recorded
424 with 50 μM [U-15N]-labeled NN206 titrated with 25 μM unlabeled denatured lysozyme. ^{1}H-^{15}N NOE data
425 were recorded in an interleaved manner: one spectrum with 4 s recycle delay followed by 4 s saturation
426 and another spectrum with no saturation and 8 s recycle delay. All NMR data were processed and
427 analyzed by XWIN-NMR (Bruker BioSpin), NMRPipe[37], and NMRView[38].

428 ***Data availability***

429 The atomic coordinates and structure factors have been deposited in the Protein Data
430 Bank, www.pdb.org, with accession codes 7CR9 and 7CRA. Other relevant data are available from the
431 corresponding author upon reasonable requests.

432

433 **References**

434 1. Charette, M.F., Henderson, G.W. & Markovitz, A. ATP hydrolysis-dependent protease
435 activity of the lon (capR) protein of Escherichia coli K-12. *Proc Natl Acad Sci U S A* **78**, 4728-
436 32 (1981).
437 2. Park, S.C. et al. Oligomeric structure of the ATP-dependent protease La (Lon) of
438 Escherichia coli. *Mol Cells* **21**, 129-34 (2006).
439 3. Goldberg, A.L., Moerschell, R.P., Chung, C.H. & Maurizi, M.R. ATP-dependent protease La
440 (lon) from Escherichia coli. *Methods Enzymol* **244**, 350-75 (1994).
441 4. Rotanova, T.V. et al. Classification of ATP-dependent proteases Lon and comparison of
442 the active sites of their proteolytic domains. *European Journal of Biochemistry* **271**, 4865-
443 4871 (2004).
444 5. Botos, I. et al. The catalytic domain of Escherichia coli Lon protease has a unique fold and
445 a Ser-Lys dyad in the active site. *Journal of Biological Chemistry* **279**, 8140-8148 (2004).
446 6. Higashitani, A., Ishii, Y., Kato, Y. & Koriuchi, K. Functional dissection of a cell-division
447 inhibitor, SulA, of Escherichia coli and its negative regulation by Lon. *Mol Gen Genet* **254**,
448 351-7 (1997).
449 7. Wohlever, M.L., Baker, T.A. & Sauer, R.T. Roles of the N domain of the AAA+ Lon protease
450 in substrate recognition, allosteric regulation and chaperone activity. *Mol Microbiol* **91**,
451 66-78 (2014).
452 8. Ebel, W., Skinner, M.M., Dierksen, K.P., Scott, J.M. & Trempy, J.E. A conserved domain in
453 Escherichia coli Lon protease is involved in substrate discriminator activity. *J Bacteriol* **181**,
454 2236-43 (1999).
455 9. Roudiak, S.G. & Shrader, T.E. Functional role of the N-terminal region of the Lon protease
456 from Mycobacterium smegmatis. *Biochemistry* **37**, 11255-63 (1998).
457 10. Rudyak, S.G. & Shrader, T.E. Polypeptide stimulators of the Ms-Lon protease. *Protein Sci*
458 **9**, 1810-7 (2000).
459 11. Iyer, L.M., Leipe, D.D., Koonin, E.V. & Aravind, L. Evolutionary history and higher order
460 classification of AAA+ ATPases. *J Struct Biol* **146**, 11-31 (2004).
461 12. Melnikov, E.E. et al. Limited proteolysis of E. coli ATP-dependent protease Lon - a unified
462 view of the subunit architecture and characterization of isolated enzyme fragments. *Acta*
463 *Biochim Pol* **55**, 281-96 (2008).
464 13. Adam, C. et al. Biological roles of the Podospora anserina mitochondrial Lon protease and
465 the importance of its N-domain. *PLoS One* **7**, e38138 (2012).

466 14. Cheng, I. et al. Identification of a Region in the N-Terminus of Escherichia coli Lon That
467 Affects ATPase, Substrate Translocation and Proteolytic Activity. *Journal of Molecular*
468 *Biology* **418**, 208-225 (2012).
469 15. Gottesman, S. Proteolysis in bacterial regulatory circuits. *Annu Rev Cell Dev Biol* **19**, 565-
470 87 (2003).
471 16. Baker, T.A. & Sauer, R.T. ATP-dependent proteases of bacteria: recognition logic and
472 operating principles. *Trends Biochem Sci* **31**, 647-53 (2006).
473 17. Lin, C.C. et al. Structural Insights into the Allosteric Operation of the Lon AAA+ Protease.
474 *Structure* **24**, 667-675 (2016).
475 18. Su, S.C. et al. Structural Basis for the Magnesium-Dependent Activation and
476 Hexamerization of the Lon AAA+ Protease. *Structure* **24**, 676-686 (2016).
477 19. Li, M. et al. Crystal structure of the N-terminal domain of E. coli Lon protease. *Protein Sci*
478 **14**, 2895-900 (2005).
479 20. Duman, R.E. & Lowe, J. Crystal structures of Bacillus subtilis Lon protease. *J Mol Biol* **401**,
480 653-70 (2010).
481 21. Li, M. et al. Structure of the N-terminal fragment of Escherichia coli Lon protease. *Acta*
482 *Crystallogr D Biol Crystallogr* **66**, 865-73 (2010).
483 22. Chen, X. et al. Crystal structure of the N domain of Lon protease from Mycobacterium
484 avium complex. *Protein Sci* **28**, 1720-1726 (2019).
485 23. Hsu, S.T., Cabrita, L.D., Fucini, P., Dobson, C.M. & Christodoulou, J. Structure, dynamics
486 and folding of an immunoglobulin domain of the gelation factor (ABP-120) from
487 Dictyostelium discoideum. *J Mol Biol* **388**, 865-79 (2009).
488 24. Van Melderen, L. et al. ATP-dependent degradation of CcdA by Lon protease. Effects of
489 secondary structure and heterologous subunit interactions. *J Biol Chem* **271**, 27730-8
490 (1996).
491 25. Yang, M., Dutta, C. & Tiwari, A. Disulfide-bond scrambling promotes amorphous
492 aggregates in lysozyme and bovine serum albumin. *J Phys Chem B* **119**, 3969-81 (2015).
493 26. Gur, E. & Sauer, R.T. Recognition of misfolded proteins by Lon, a AAA(+) protease. *Genes*
494 *Dev* **22**, 2267-77 (2008).
495 27. Patterson, J. et al. Correlation of an adenine-specific conformational change with the ATP-
496 dependent peptidase activity of Escherichia coli Lon. *Biochemistry* **43**, 7432-42 (2004).
497 28. Vasilyeva, O.V., Kolygo, K.B., Leonova, Y.F., Potapenko, N.A. & Ovchinnikova, T.V. Domain
498 structure and ATP-induced conformational changes in Escherichia coli protease Lon
499 revealed by limited proteolysis and autolysis. *FEBS Lett* **526**, 66-70 (2002).
500 29. McCoy, A.J., Fucini, P., Noegel, A.A. & Stewart, M. Structural basis for dimerization of the
501 Dictyostelium gelation factor (ABP120) rod. *Nat Struct Biol* **6**, 836-41 (1999).
502 30. Wernimont, A. & Edwards, A. In situ proteolysis to generate crystals for structure
503 determination: an update. *PLoS One* **4**, e5094 (2009).
504 31. Otwinowski, Z. & Minor, W. [20] Processing of X-ray diffraction data collected in
505 oscillation mode. *Methods Enzymol* **276**, 307-326 (1997).
506 32. McCoy, A.J. Solving structures of protein complexes by molecular replacement with
507 Phaser. *Acta Crystallogr D Biol Crystallogr* **63**, 32-41 (2007).

508 33. Terwilliger, T.C. et al. Iterative model building, structure refinement and density
509 modification with the PHENIX AutoBuild wizard. *Acta Crystallogr D Biol Crystallogr* **64**, 61-
510 9 (2008).
511 34. Emsley, P. & Cowtan, K. Coot: model-building tools for molecular graphics. *Acta*
512 *Crystallogr D Biol Crystallogr* **60**, 2126-32 (2004).
513 35. Murshudov, G.N. et al. REFMAC5 for the refinement of macromolecular crystal structures.
514 *Acta Crystallogr D Biol Crystallogr* **67**, 355-67 (2011).
515 36. Sattler M, S.J., Griesinger C. Heteronuclear multidimensional NMR experiments for the
516 structure determination of proteins in solution employing pulsed field gradients. *Progress*
517 *in Nuclear Magnetic Resonance Spectroscopy.* **34**, 93-158 (1999).
518 37. Delaglio, F. et al. NMRPipe: a multidimensional spectral processing system based on UNIX
519 pipes. *J Biomol NMR* **6**, 277-93 (1995).
520 38. Downing, A.K. *Protein NMR techniques*, xi, 487 p. (Humana Press, Totowa, N.J., 2004).
521

522 **Acknowledgements**

523 We thank Dr. Shang-Te Danny Hsu for helpful discussion. We also thank Ms S.-L. Huang of
524 Ministry of Science and Technology (National Taiwan University) for the assistance in NMR experiments.
525 We are grateful to the staff of the Biomedical Resource Core at the First Core Labs, National Taiwan
526 University College of Medicine, for technical assistance. Portions of this research were carried out at
527 beamlines 13B1 and 13C1 of the National Synchrotron Radiation Research Center (Taiwan). This work
528 was supported by National Taiwan University Grants 108L7809 and 109L7809; and the Ministry of
529 Science and Technology, Taiwan (grant numbers: MOST108-2113-M-002-006- and MOST109-2113-M-
530 002-018- to S.-R.T. and MOST105-2320-B-001-015-MY3 to C.-I.C.).
531

532 **Author contributions**

533 S.R.T., and C.I.C. conceived the study. S.R.T., and C.I.C. designed the experiments and analyzed the
534 data. Y.C.T., C.C.L., Y.T.K., and S.J.H. performed the experiments. S.R.T., and C.I.C. wrote the
535 manuscript with inputs from all other authors.
536
537
538
539
540
541
542
543
544

545

546 **Table 1.** Data collection and refinement statistics

	NN206	NN291
PDB entry	7CR9	7CRA
Data collection		
Space group	P212121	P6322
Cell dimensions		
a, *b*, *c* (Å)	32.830, 58.296, 198.492	86.016, 86.016, 110.126
α, β, γ (°)	90, 90, 90	90, 90, 120
Resolution (Å)	30 - 2.09 (2.16 - 2.09)*	30 - 1.7 (1.76 - 1.7)
R_{sym} or R_{merge}	0.106 (0.937)	0.069 (0.779)
$I/\sigma I$	17.9 (3.0)	49.1 (4.7)
Completeness (%)	99.7 (100)	100 (100)
Redundancy	6.5 (6.6)	20.9 (21.4)
Refinement		
Resolution (Å)	29.409 - 2.1 (2.149 -2.1)	30 - 1.7 (1.744 - 1.7)
R_{work}/ R_{free}	0.209/0.249	0.197/0.237
No. atoms		
Protein	3285	1684
Ligand (SO_4^{2-})	0	10
Water	107	244
B-factors		
Protein	53.14	16.18
Ligand (SO_4^{2-})		27.45
Water	52.66	28.21
R.m.s deviations		
Bond lengths (Å)	0.004	0.009
Bond angles (º)	0.74	1.34
Ramachandran		
Favored (%)	96.81	96.67
Allowed (%)	2.46	2.38
Outliers (%)	0.74	0.95

547 Number of crystals for each structure should be noted in footnote.
548 *Highest resolution shell is shown in parenthesis.
549

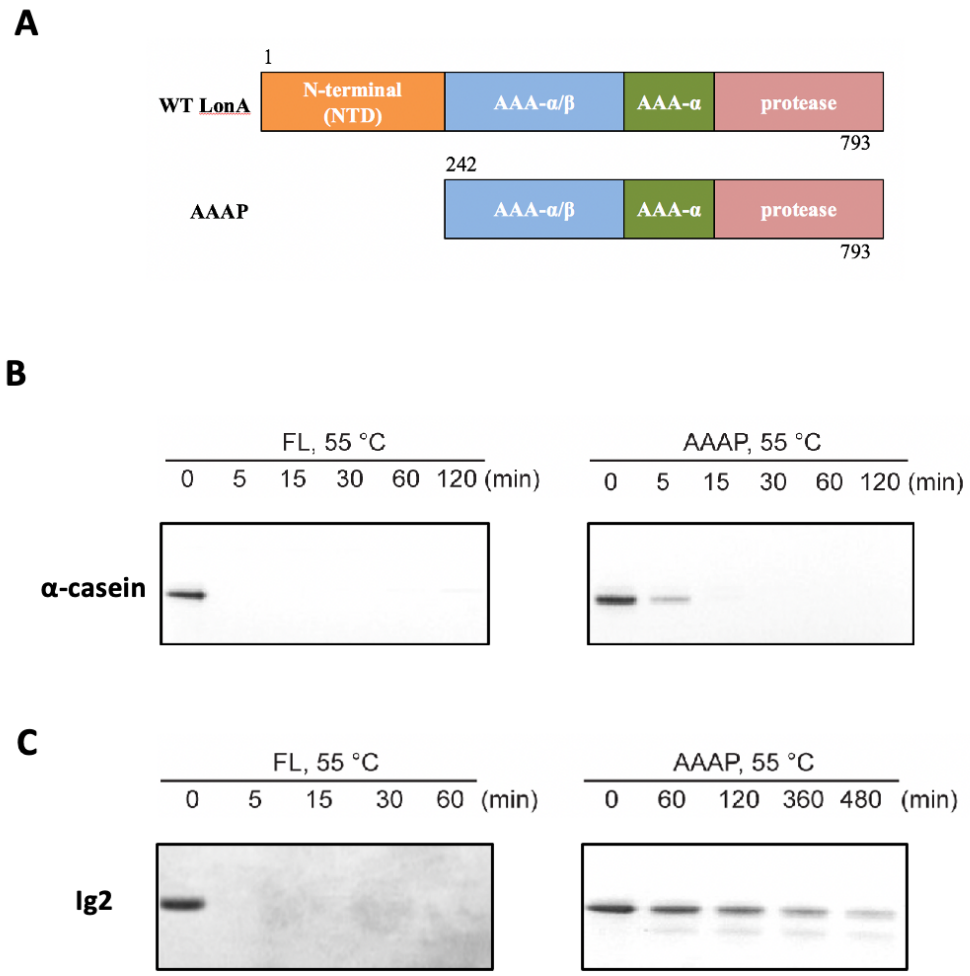

Fig. 1. ***The NTD of Meiothermus taiwanensis LonA (MtaLonA) is essential for efficient degradation of a thermally unfolded substrate, but not the intrinsically disordered substrate, α-casein.*** (A) Schematic diagrams illustrating domain organization of full-length MtaLonA and the N-terminal domain truncated AAAP. (B) Degradation of α-casein by full-length MtaLonA (FL) and AAAP at 55 °C. (C) Degradation of Ig2 by full-length and AAAP at 55 °C.

557

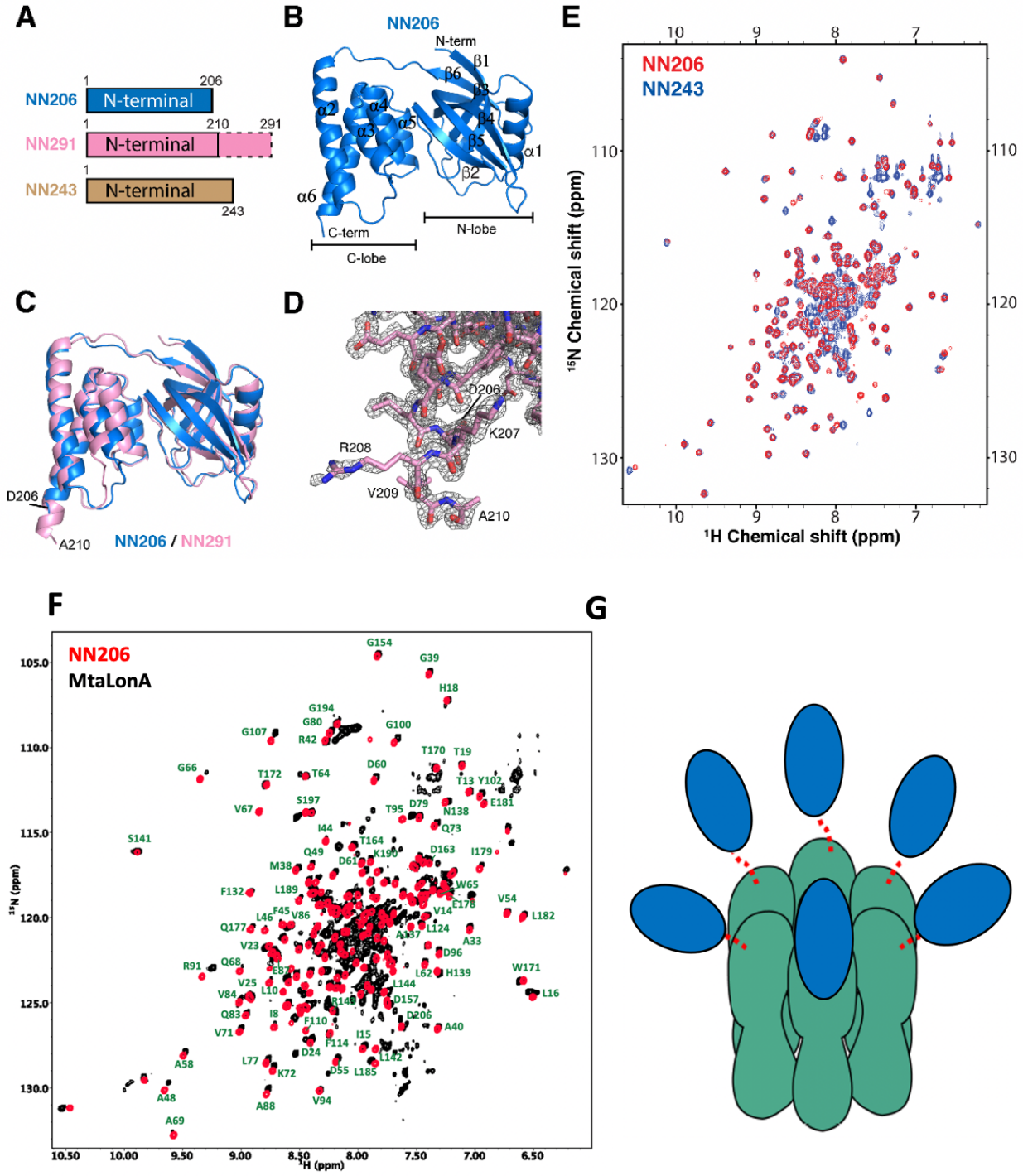

558

559 Fig. 2. ***Overall structures of the N-terminal domain of MtaLonA.*** (A) The three N-terminal
560 constructs NN206, NN291, and NN243. The disordered region is shown in the dashed box. (B)
561 Structure of NN206. (C) Superposition of NN206 (marine) and NN291 (pink) structures.

562 *Figure 2 continued on next page*

563 *Figure 2 continued*

564 (D) The refined *2F0-Fc* electron density map around the C-terminal residue A210 of NN291,
565 contoured at 1.0 σ. (E) Overlay of 2D $^{1}H–^{15}N$ HSQC NMR spectra of NN206 (red) and NN243
566 (blue). (F) Comparison of the $^{1}H–^{15}N$ TROSY HSQC spectra of NN206 (red) and MtaLonA
567 (black) recorded at 55 °C. The well-dispersed resonances are labeled with residue numbers.
568 About 200 well-resolved correlations are superimposable, suggesting that NTD is loosely linked
569 to the hexameric core via a flexible linker. (G) The six NTD may each connect to the hexameric
570 core of fused AAA+ and protease domains by a flexible ~40-residue linker. The NTDs, and
571 ATPase-Protease chamber are illustrated in blue and green colors, respectively. Red dashed lines
572 represent the flexible linker regions.
573
574
575
576
577
578
579
580
581
582
583
584
585
586
587
588
589
590
591
592
593

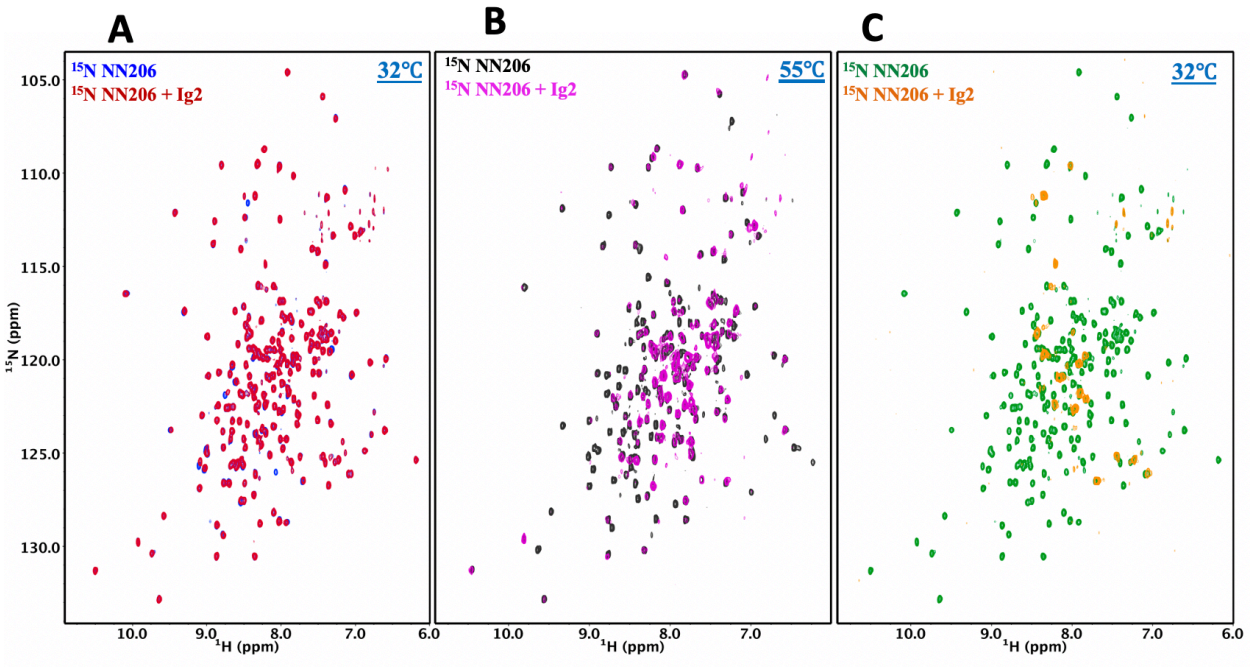

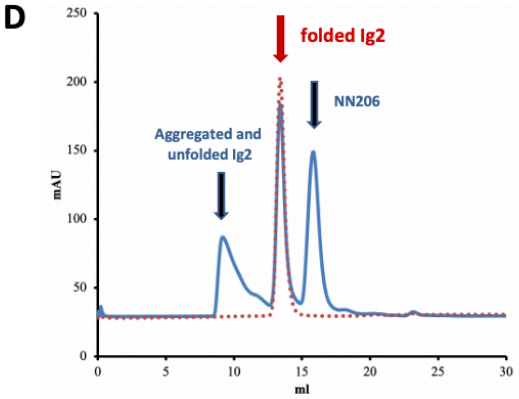

Fig. 3. ***The N-lobe of MtaLonA NTD is involved in recognition of thermally unfolded substrate Ig2.*** (A) ^{1}H–^{15}N TROSY HSQC spectra of NTD in the absence (blue) and presence (red) of Ig2 recorded at 32 °C. (B) Comparison of the ^{1}H–^{15}N TROSY HSQC spectra of NN206 in the apo (black) and Ig2-bound (magenta) states recorded at 55 °C. (C) After one thermal cycle, ^{1}H–^{15}N TROSY HSQC spectra of NTD in the absence (green) and presence (orange) of Ig2 recorded at 32 °C. (D) Gel filtration profiles of NMR samples treated with thermal cycling shown in blue, and folded Ig2 (red) analyzed by Superdex 200 10/300 GL column.

Figure 3 continued on next page

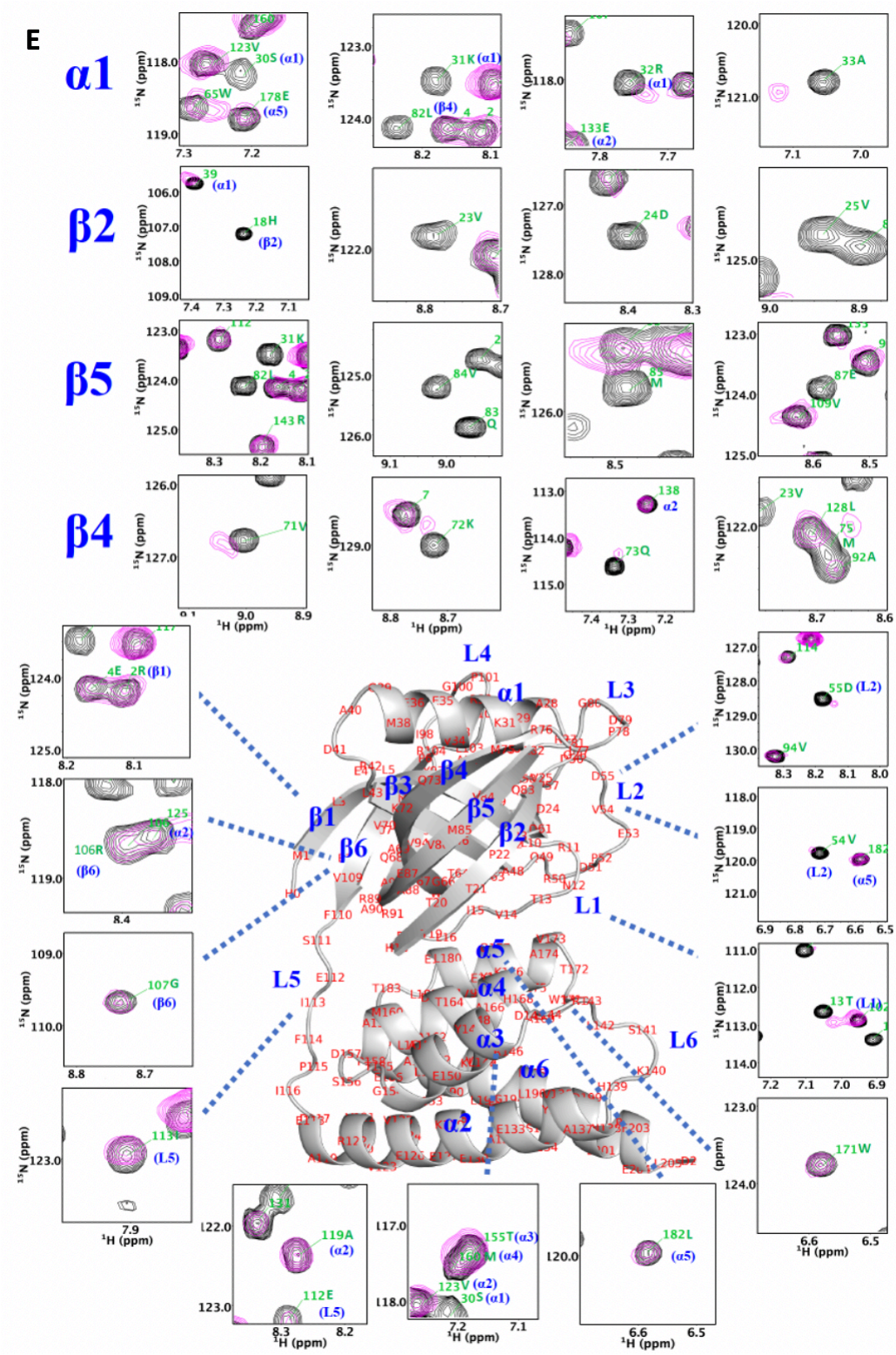

605 (E) Comparison of the ^{1}H–^{15}N TROSY HSQC spectra of NN206 in the apo (black) and Ig2-bound
606 (magenta) states. The residues of NTD with the CSPs are part of the interaction interface, located
607 mainly at β-sheet β2/β5/β4, loop L1, L2, L3 and helix α1. *Figure 3 continued on next page*

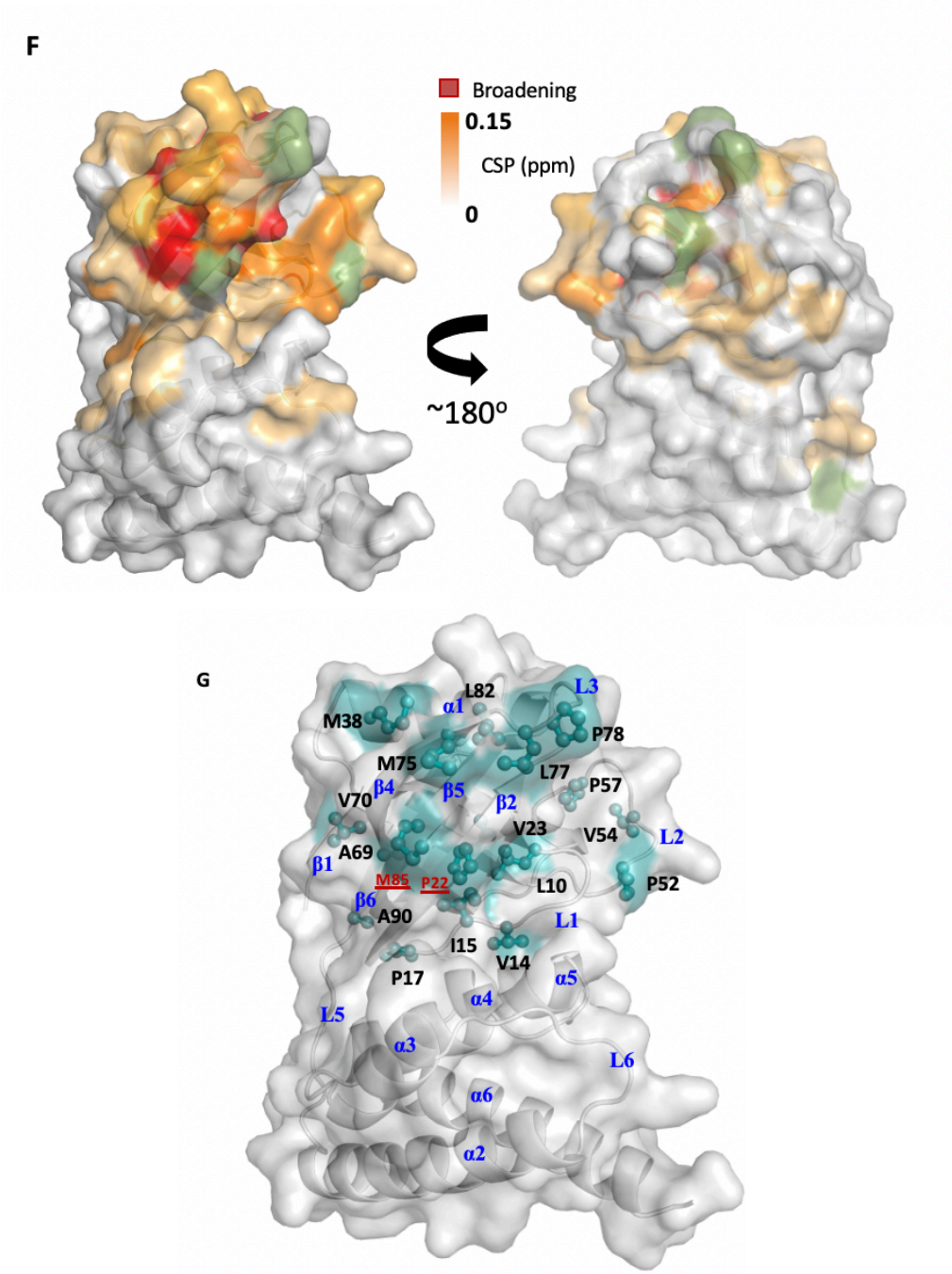

(F) Interaction interface of NTD: Ig2 mapped onto the structure of NTD, based on the spectrum recorded at 55 °C. Proline residue is shown in green. (G) The exposed hydrophobic residues that make up the damaged Ig2-binding sites are shown as balls and sticks. Mutations of two exposed hydrophobic residues P22 and M85, located at the center of β-sheet β2/β5/β4, lead to reduce the hydrophobicity of the contiguous hydrophobic surface in the N-lobe subdomain.

Figure 3 continued on next page

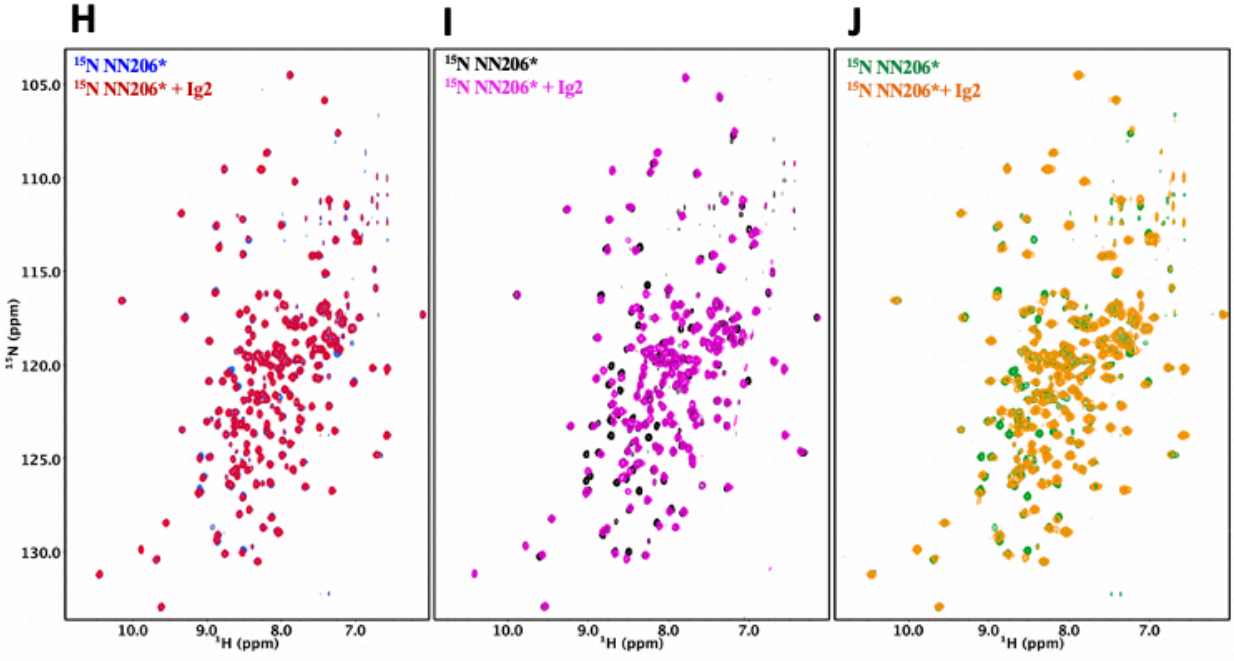

Figure 3 continued

(H) ^{1}H–^{15}N TROSY HSQC spectra of NTD* (blue) in the absence (blue) and presence (red) of Ig2 recorded through thermal cycling from 32 °C (H) to 55 °C (I) and then returning to 32 °C (J).

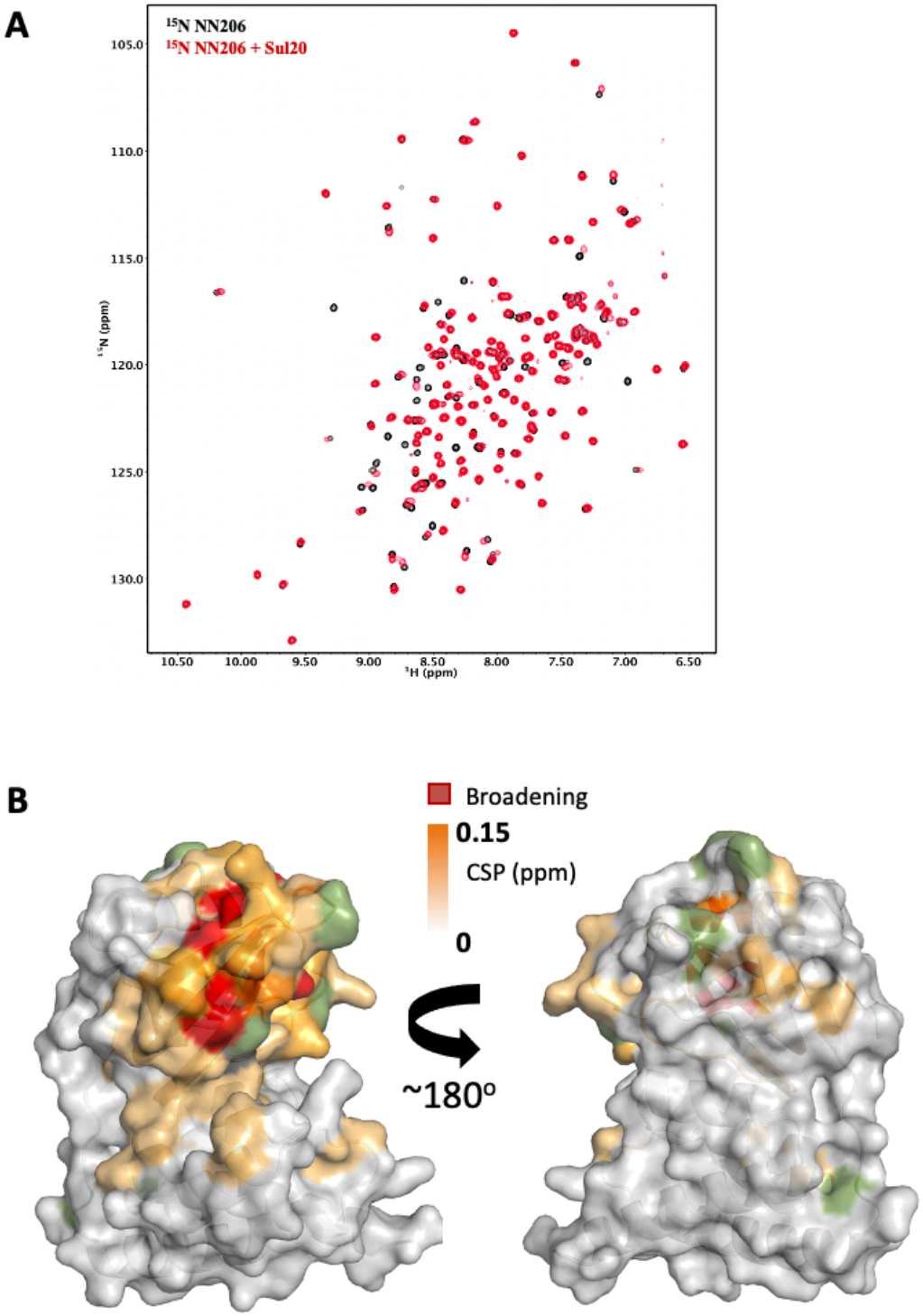

Fig. 4. ***Interaction of MtaLonA NTDs with degron tag Sul20.*** (A) Overlay of the ^{1}H–^{15}N TROSY HSQC spectra of NN206 in the absence (black) and presence (red) of Sul20 peptide. (B) Structural mapping of the chemical shift perturbations (orange) of NN206 caused by Sul20 peptide.

Figure 4 continued on next page

Figure 4 continued

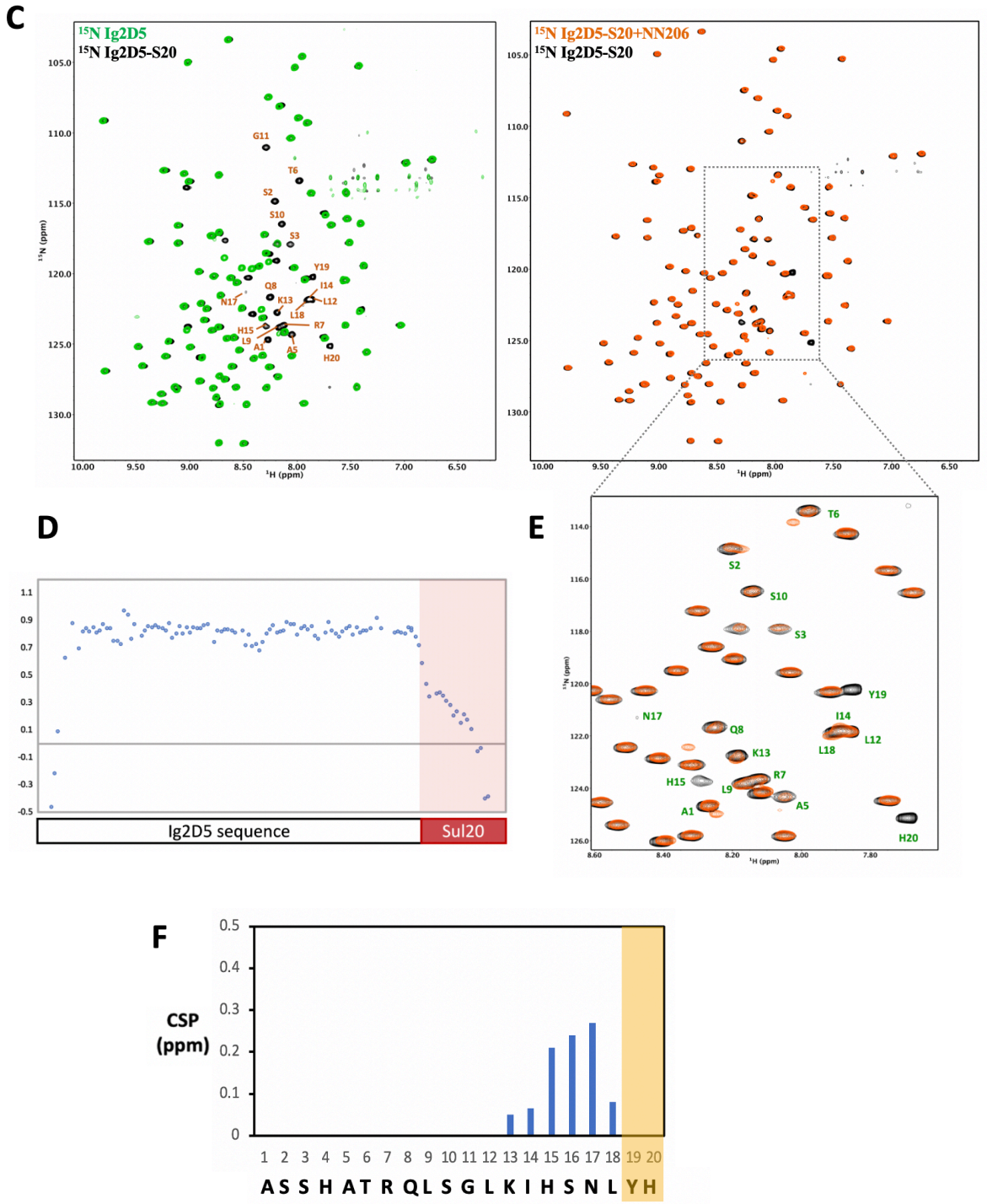

(C) Overlay of the ^{1}H–^{15}N TROSY HSQC spectra of Ig2D5 (green) and Ig2D5-S20 (black); overlay of the ^{1}H–^{15}N TROSY HSQC spectra of Ig2D5-S20 in the absence (black) and in the presence (orange) of an equimolar amount of NN206. (D) [^{1}H]–^{15}N nuclear Overhauser effect

628 (NOE) values of Ig2D5-S20. (E) Expanded region of the $^{1}H–^{15}N$ TROSY HSQC spectra of Ig2D5-
629 S20 in the absence (black) and in the presence (orange) of NN206. (F) CSPs of amide moieties of
630 50 μM Ig2D5-S20 after binding 50 μM unlabeled NN206, plotted against Sul20 residue number.
631 Residues Y19 and H20 are strongly affected by the binding event based on the resonance
632 broadening beyond detection.
633
634
635
636

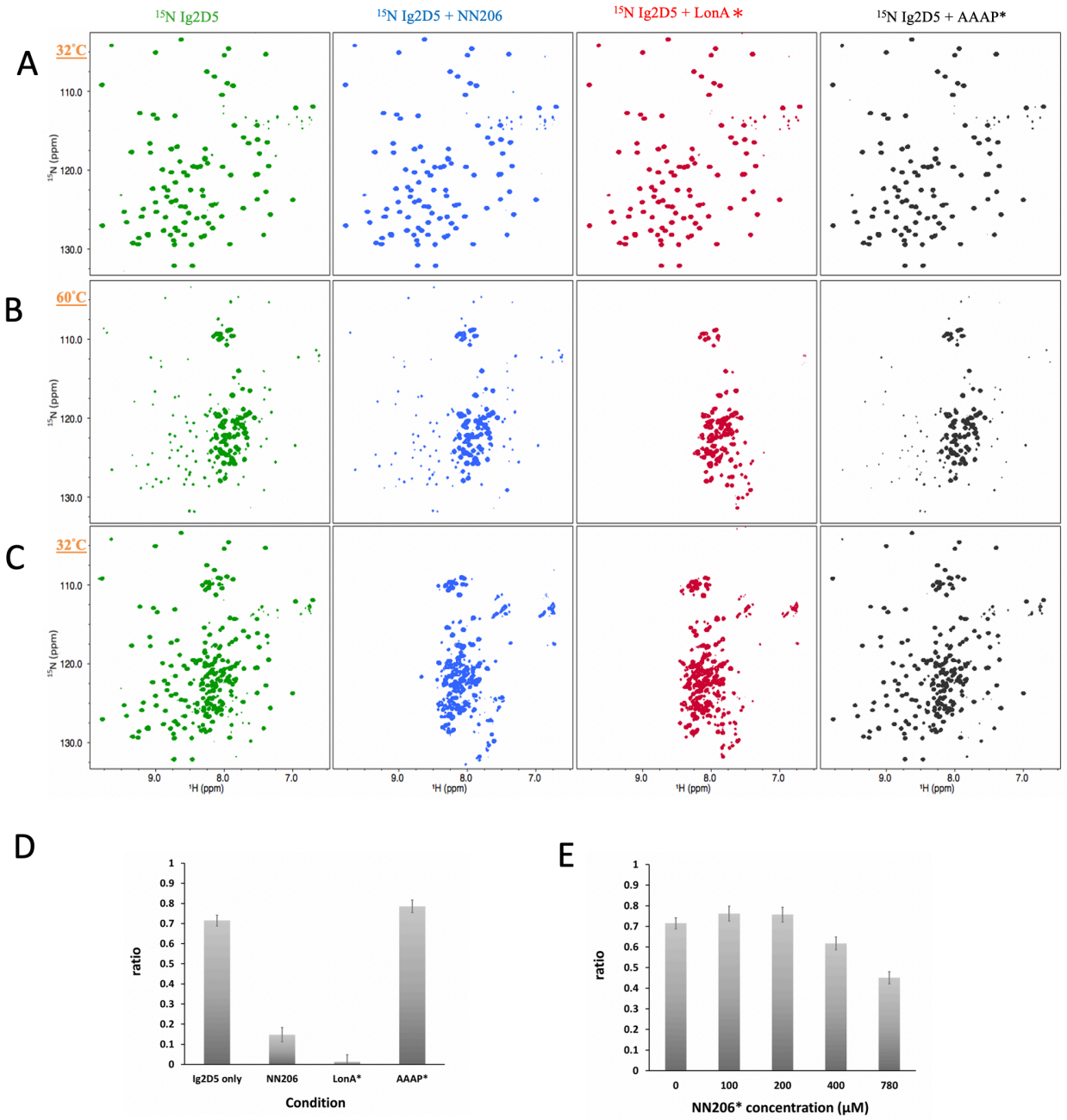

637

638 Fig. 5. ***The thermodynamics of Ig2D5 unfolding-refolding is affected in the presence of***
639 ***MtaLonA NTDs.*** 2D ^{1}H-^{15}N TROSY HSQC NMR spectra of apo Ig2D5(green), Ig2D5 titrated
640 with NN206(blue), LonA (red), or AAAP (black) are recorded with a thermal cycle starting from
641 32 °C (A) to 60 °C (B), and then returning to 32 °C (C). (D) Folded ratio of apo Ig2D5, Ig2D5
642 titrated with NN206(blue), LonA (red), or AAAP (black) after a thermal cycle. (E) Folded ratio
643 of apo Ig2D5, Ig2D5 titrated with different concentrations of NN206* after one thermal cycle.

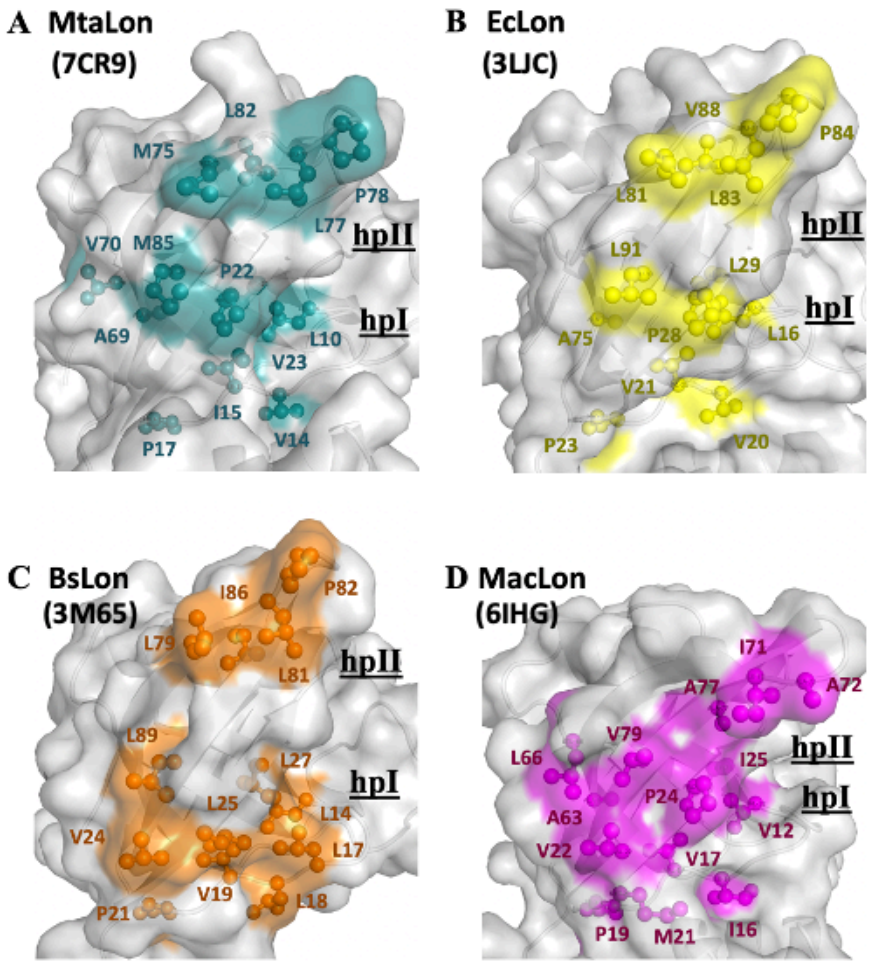

644

645 Fig. 6 ***The NTD of MtaLonA selectively interacts with unfolded proteins, protein aggregates,***
646 ***and degron-tagged proteins via two hydrophobic patches of its N-lobe.*** (A) Two hydrophobic
647 patches located at the N-lobe of MtaLonA: (i) Leu-10, Ile-15, Pro-22, Val-23, and Met-85
648 (termed hpI in the following); (ii) Met-75, Leu-77, Pro-78 and Leu-82 (termed hpII). (B) Hp I
649 and II of EcLonA: (i) Leu-16, Val-21, Pro-28, Leu-29, and Leu-91; (ii) Leu-81, Leu-83, Pro-84
650 and Val-88. (C) Hp I and II of BsLonA: (i) Leu-14, Leu-17, Leu-18, Val-19, Val-24, Leu-25,
651 Leu-27 and Leu-89; (ii) Leu-79, Leu-81, Pro-82 and Ile-86. (D) merged Hp I and II of
652 MacLonA: (i) Val-12, Val-17, Val-22, Pro-24, Ile-25, Leu-66 and Val-79; (ii) Ile-71, Ala-72 and
653 Ala-77. The conserved hydrophobic patches at the N-lobes may be potentially responsible for
654 conferring substrate selectivity toward degrons, misfolded and damaged proteins. The PDB
655 codes are indicated in parentheses.

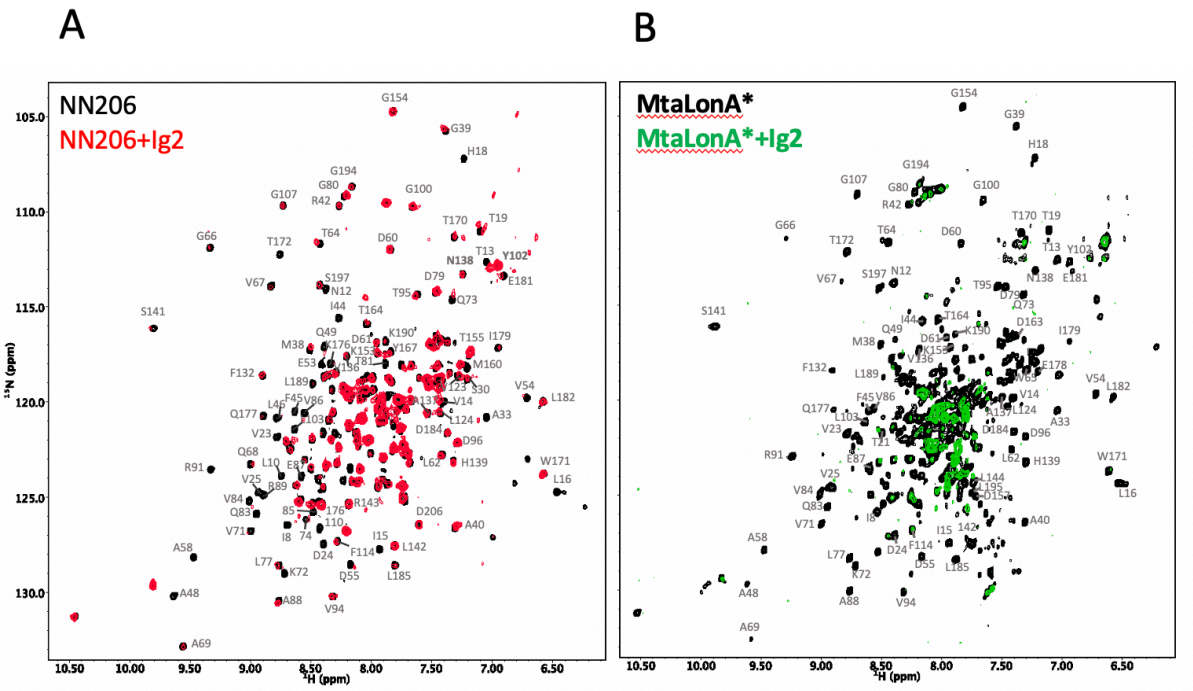

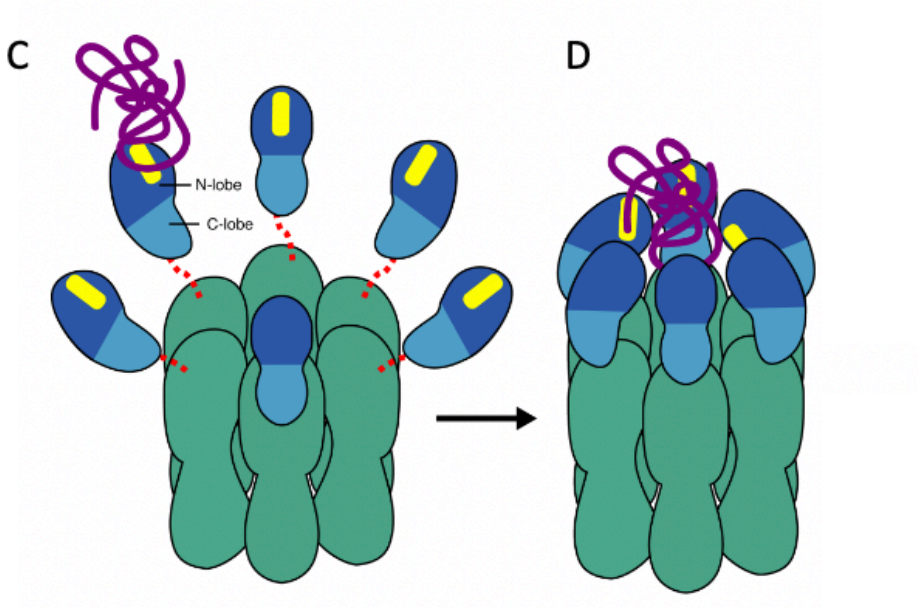

Fig. 7. ***Proposed model for NTD-mediated substrate interaction.***
(A) ^{1}H–^{15}N TROSY HSQC spectra of NTD in the absence (black) and presence (red) of unlabeled Ig2 recorded at 55 °C. (B) ^{1}H–^{15}N TROSY HSQC spectra of LonA* in the absence (black) and presence (green) of unlabeled Ig2 recorded at 55 °C. (C) The flexibly linked NTD of the hexametric LonA is swaying from side to side and back and forth to survey, recognize, and trap substrates with exposed hydrophobic sequences. Substrate, N-lobe, Clobe of NTDs, and the

664 ATPase-Protease chamber are illustrated in purple, marine, blue and green colors, respectively.
665 The substrate-binding patches are depicted in yellow. Red dashed lines represent the flexible
666 linker regions. (D) After initial binding, other NTDs may join to increase the avidity of the
667 LonA-substrate interaction. The substrate polypeptide chain is pulled inside the chamber and
668 undergoes proteolysis by protease modules of LonA.